Section Editor: **Alexander Zarbock**

Glycocalyx Degradation Is Independent of Vascular Barrier Permeability Increase in Nontraumatic Hemorrhagic Shock in Rats

Philippe Guerci, MD,*†‡ Bulent Ergin, PhD,*§ Zuhre Uz, MD,* Yasin Ince, MSc,* Martin Westphal, MD, PhD,‖ Michal Heger, PhD,¶ and Can Ince, PhD*§

BACKGROUND: Glycocalyx shedding after traumatic hemorrhagic or septic shock, as well as different resuscitation fluids, has been causally linked to increased vascular barrier permeability (VBP) resulting in tissue edema. In nontraumatic hemorrhagic shock (NTHS), it remains questionable whether glycocalyx degradation in itself results in an alteration of VBP. The composition of fluids can also have a modulatory effect on glycocalyx shedding and VBP. We hypothesized that the shedding of the glycocalyx during NTHS has little effect on VBP and that the composition of fluids can modulate these effects.

METHODS: Fully instrumented Wistar-albino rats were subjected to a pressure-controlled NTHS (mean arterial pressure of 30 mm Hg) for 60 minutes. Animals were fluid resuscitated with Ringer's acetate, balanced hydroxyethyl starch (HES) solution, or 0.9% normal saline to a mean arterial pressure of 80 mm Hg and compared with shams or nonresuscitated NTHS. Glycocalyx shed products were determined at baseline and 60 minutes after fluid resuscitation. Skeletal muscle microcirculation was visualized using handheld vital microscopy. VBP changes were assessed using plasma decay of 3 fluorescent dyes (40- and 500-kDa dextran and 70-kDa albumin), Evans blue dye exclusion, intravital fluorescence microscopy, and determination of tissue edema (wet/dry weight ratio).

RESULTS: All glycocalyx shedding products were upgraded as a result of NTHS. Syndecan-1 significantly increased in NTHS (mean difference, −1668; 95% confidence interval [CI], −2336 to −1001; $P < .0001$), balanced crystalloid (mean difference, −964.2; 95% CI, −1492 to −436.4; $P = .0001$), and HES (mean difference, −1030; 95% CI, −1594 to −465.8; $P = .0001$) groups at the end of the experiment compared to baseline. Hyaluronan levels were higher at the end of the experiment in nonresuscitated NTHS (−923.1; 95% CI, −1216 to −630; $P = .0001$) and balanced crystalloid (−1039; 95% CI, −1332 to −745.5; $P = .0001$) or HES (−394.2; 95% CI, −670.1 to −118.3; $P = .0027$) groups compared to controls. Glycocalyx shedding resulted in microcirculation alterations as observed by handheld video microscopy. Total vessel density was altered in the normal saline (mean difference, 4.092; 95% CI, 0.6195–7.564; $P = .016$) and hemorrhagic shock (mean difference, 5.022; 95% CI, 1.55–8.495; $P = .0024$) groups compared to the control group, as well as the perfused vessel density and mean flow index. Despite degradation of endothelial glycocalyx, VBP as determined by 4 independent assays remained intact and continued to be so following fluid resuscitation.

CONCLUSIONS: NTHS induced glycocalyx shedding and microcirculation alterations, without altering VBP. Fluid resuscitation partially restored the microcirculation without altering VBP. These results challenge the concept that the glycocalyx barrier is a significant contributor to VBP. (Anesth Analg 2019;129:598–607)

KEY POINTS

- **Question:** Is glycocalyx degradation occurring during nontraumatic hemorrhage followed by fluid resuscitation of different composition associated with a degradation of the vascular barrier?
- **Finding:** Glycocalyx degradation occurs during nontraumatic hemorrhagic shock but without affecting vascular barrier permeability and is not prevented by fluids of different composition.
- **Meaning:** Increase in vascular barrier permeability seen in states of perioperative and critical illness requires compromise of other barrier constituents, such as cell-to-cell junctions, compared with solely glycocalyx shedding.

From the *Department of Translational Physiology, Academic Medical Center, University of Amsterdam, Amsterdam, the Netherlands; †Institut National de la Santé et de la Recherche Médicale U1116, University of Lorraine, Vanoeuvre-Les-Nancy, France; ‡Department of Anesthesiology and Critical Care Medicine, University Hospital of Nancy, Vandoeuvre-Les-Nancy, France; §Department of Intensive Care Medicine, Erasmus MC, University Medical Center Rotterdam, Rotterdam, the Netherlands; ‖Fresenius Kabi Deutschland GmbH, Bad Homburg, Germany; and ¶Department of Experimental Surgery, Academic Medical Center, University of Amsterdam, Amsterdam, the Netherlands.

Accepted for publication October 8, 2018.

Funding: This study has been supported in part by Fresenius Kabi. This study has also been supported by funds from the Department of Translational Physiology, Academic Medical Center, Amsterdam, the Netherlands. P.G. is supported by a grant from the Société Française d'Anesthésie et de Réanimation.

Conflicts of Interest: See Disclosures at the end of the article.

Supplemental digital content is available for this article. Direct URL citations appear in the printed text and are provided in the HTML and PDF versions of this article on the journal's website (www.anesthesia-analgesia.org).

P. Guerci and B. Ergin contributed equally and share first authorship.

Reprints will not be available from the authors.

Address correspondence to Philippe Guerci, MD, Department of Translational Physiology, Academic Medical Center, University of Amsterdam, Meibergdreef 9, 1105 AZ Amsterdam, the Netherlands. Address e-mail to phil.guerci@gmail.com.

DOI: 10.1213/ANE.0000000000003918

The vascular barrier is mainly composed of the glycocalyx, endothelial cells, and cell-to-cell junctions.[1–3] The main functions of the glycocalyx are to protect the endothelium, facilitate numerous physiological processes, and regulate cellular and macromolecular traffic.[4] Degradation of the glycocalyx has been associated as a key step in the pathogenesis of a large number of cardiovascular diseases, such as shock,[5,6] sepsis,[7,8] diabetes,[9] atherosclerosis,[10] heart failure, and volume overload.[11]

One of the main implicit assumptions in the literature has been that the glycocalyx barrier is the key vascular component defining vascular barrier permeability (VBP)[3] and that its disruption is the primary cause of vascular leakage causing tissue edema. However, the causal relationship between glycocalyx degradation and vascular barrier breakdown has not been clearly demonstrated. Studies that have demonstrated glycocalyx shedding in various experimental and clinical settings have not demonstrated that glycocalyx shedding in itself produces an increase in VBP.[12–15] Other experimental studies performed on glycocalyx degradation have used interventions, such as enzymatic degradation,[16–19] not often seen in clinical conditions, which, other than the glycocalyx, could also disrupt other components associated with VBP, such as endothelial cell integrity and endothelial cell-to-cell junctions leading to capillary leakage.

This uncertainty has led us to formulate the hypothesis that in nontraumatic hemorrhagic shock (NTHS), such as can occur during the perioperative phase, glycocalyx degradation can indeed occur but without the negative consequences of VBP alterations and that this degradation might not be the primary component responsible for VBP alterations associated with edema. In extension to this hypothesis, we assumed that fluid resuscitation may influence components of the glycocalyx but may not result in deleterious effects on VBP, indicating that fluid therapy is a safe and effective therapy during NTHS.

In the present study, we proposed to induce NTHS and investigate these issues. To demonstrate that the intervention of glycocalyx shedding has been achieved, we intended to measure the presence of shedding products of the glycocalyx in plasma and to use direct imaging of the microcirculation using a handheld vital microscope to analyze microcirculatory disturbances known to be associated with the endothelial glycocalyx degradation.[9,20]

In doing so, we proposed to investigate whether the NTHS-induced glycocalyx shedding in the rat model resulted in an alteration in VBP. To this end, we used 4 independent assays for the measurement of VBP: (1) analysis of plasma decay of fluorescence dyes of different molecular sizes; (2) extravasation of Evans blue dye in organs; (3) observation of fluorescent dye extravasation in microvessels by intravital fluorescence microscopy; and (4) edema formation in organs measured by water content (wet/dry weight ratio). The reason we chose these 4 independent methodologies to measure VBP was to provide a solid base of evidence as to the presence or absence of vascular leakage in our model. Using this approach, we proposed to provide comprehensive evidence as to the effects of glycocalyx degradation on VBP and its possible modulation by the use of fluid resuscitation of different compositions.

METHODS

Animals

This study was approved by the Animal Research Committee of the Academic Medical Center of the University of Amsterdam (DFL 190AA). Care and handling of the animals were in accordance with the guidelines from the Institutional Animal Care and Use Committees. This manuscript adheres to the applicable Animal Research: Reporting of In Vivo Experiments guidelines. Experiments were performed on male Wistar-albino rats (Charles River Laboratories, Den Bosch, the Netherlands), 10 ± 2 weeks of age, with a mean ± standard deviation (SD) body weight (BW) of 334 ± 24 g.

Surgical Preparation

The rats (n = 59) were anesthetized with an intraperitoneal injection of 100 mg·kg^{-1} ketamine (Nimatek; Eurovet, Bladel, the Netherlands), 0.5 mg·kg^{-1} medetomidine (Domitor; Pfizer, Bladel, the Netherlands), and 0.05 mg·kg^{-1} atropine sulfate (Centrafarm, Bladel, the Netherlands). Anesthesia was maintained with 50 mg·kg·hour^{-1} ketamine. Fluid maintenance consisted of Ringer's acetate (Baxter, Utrecht, the Netherlands) at a rate of 10 mL·kg^{-1}·hour^{-1}. After a tracheostomy, the animals were connected to a ventilator (Babylog 8000; Dräger Nederland, Bladel, the Netherlands) and ventilated with tidal volumes of 6 mL·kg^{-1} with a positive end-expiratory pressure of 3 cm H_2O and an F_{IO_2} of 0.4. A heating pad under the animal allowed the body temperature to be controlled and maintained at 37°C ± 0.5°C. The end-tidal P_{CO_2} was maintained between 30 and 35 mm Hg (CapnoMac, Datex-Ohmeda; GE-Healthcare, Eindhoven, the Netherlands).

The right carotid (pressure) and left femoral (for blood shedding and samples) arteries and jugular (anesthesia and fluid maintenance) and femoral (fluid resuscitation) veins were cannulated with polyethylene catheters (outer diameter = 0.9 mm; B-Braun, Melsungen, Germany). The right biceps femoris was exposed, and the femoral artery blood flow was monitored with a transonic flowmeter probe (0.5 mm, T206; Transonic Systems Inc, Elsloo, the Netherlands). To prevent muscle desiccation, the exposed area was protected with a humidified gauze with warm 0.9% normal saline (NaCl). The bladder was catheterized via a mini-midline incision with a polyethylene tube (outer diameter = 1.2 mm) and a homemade tip to prevent spontaneous displacement and traumatic lesions. The urine output was quantified.

Experimental Protocol

Animals were randomized according to a unique code generated by an Internet website (https://www.sealedenvelope.com). On the day of experiment, a technician prepared the resuscitation fluid according to the generated code (Supplemental Digital Content 1, Figure 1, http://links.lww.com/AA/C640).

After a 30-minute stabilization period, baseline (BL) values were recorded, and arterial blood gas was assessed (ABLFlex 80; Radiometer, Copenhagen, Denmark). Hemorrhagic shock was induced by withdrawing blood at a rate of 0.5 mL·minute^{-1} using a syringe pump (Harvard Apparatus, Cambridge, MA) until a mean arterial pressure (MAP) of 30 mm Hg was maintained for 1 hour (T1) by reinfusing or withdrawing blood. After this period, animals

were left unresuscitated (hemorrhagic shock group) or resuscitated with either balanced crystalloid (Ringer's acetate) or normal saline (0.9% NaCl), or balanced hydroxyethyl starch (HES) (Volulyte HES 130/0.4, all solutions from Fresenius Kabi, Bad Homburg, Germany) was started (T2 at 15 minutes) to maintain the MAP at 80 mm Hg for 1 hour (T3). Control-instrumented animals (sham) underwent surgical preparation of the limb but were neither hemorrhaged nor resuscitated. We deliberately chose a target of 80 mm Hg because BL MAP was higher in healthy rats than in healthy humans.

Biomarkers of Glycocalyx Shedding

Syndecan-1, heparan sulfate, and hyaluronan were used as indirect makers of glycocalyx degradation. Plasma samples were stored at −20°C and were thawed and analyzed using commercial enzyme-linked immunoabsorbent assay (ELISA) kits according to the manufacturer's instructions: DuoSet Hyaluronan (DY3614; R&D Systems, Minneapolis, MN), Syndecan-1/CD138 (SCD1) ELISA kit (Cusabio Biotech Co, Ltd, Wuhan, China), and heparan sulfate proteoglycan 2 (HSPG2) ELISA kit (Cusabio Biotech Co, Ltd, Wuhan, China).

Skeletal Muscle Microcirculatory Measurements

Glycocalyx degradation results in alterations in microcirculatory perfusion, which can be observed using handheld video microscopy.[9] Incident dark field–based handheld video microscopy CytoCam (Braedius Scientific, Huizen, the Netherlands) was placed on the surface of the exposed biceps femoris.[21] Briefly, the incident dark field imaging technique uses green polarized light that is produced from a ring of circumferential light-emitting diodes that is transmitted to the tissue and absorbed by hemoglobin, thus appearing dark on images. The imaging results in sharp contour visualization of the microcirculation, showing flowing erythrocytes and leukocytes. Continuous monitoring of the same microcirculatory spot was performed with the help of a micromanipulator. One hundred frame clips (100 seconds) were recorded at every time point. All clips obtained were randomly anonymized and analyzed in a blinded fashion (group and time point). The analysis of the microvasculature was performed at BL and T3 with AVA 3.2 (Microvision Medical, Amsterdam, the Netherlands) for total vessel density (TVD), perfused vessel density (PVD), and the mean flow index (MFI) by 2 trained and independent operators (Z.U. and Y.I.), as described elsewhere.[22]

Assessment of VBP

Fluorescent Tracers. The time-dependent plasma concentration of different size fluorescent tracer molecules in plasma can be used to measure the permeability of vascular barrier, because smaller molecules will decay faster than larger tracer molecules.[9] Degradation of the vascular barrier will lead to enlargement of the protein sieving that translates in a faster plasma decay (transendothelial escape) of larger molecules. At the end of the experiment, fluid resuscitation and maintenance were stopped. Three fluorescent dyes conjugated with different sizes of molecules and dissolved in saline were thoroughly mixed together and injected intravenously by hand over 1 minute: Texas Red-40 kDa dextran (10 mg/mL, D1829, Molecular Probes; ThermoFisher Scientific, Breda, the Netherlands), Albumin-Alexa 680 (5 mg/mL, A34787, Molecular Probes; ThermoFisher Scientific), and fluorescein isothiocyanate (FITC)-500 kDa dextran (10 mg/mL, MFCD00131092; Sigma-Aldrich, Zwijndrecht, the Netherlands) (100 µL each). Blood samples (200 µL) were withdrawn at 2, 5, 10, 15, 20, 25, and 30 minutes to obtain the decay in plasma concentration of the dyes, as we had researched previously.[9] Plasma concentrations were measured for each dye in a 96-well plate fluorometer (ClarioStar; BMG LabTech, Ortenberg, Germany) in accordance with the excitation/emission wavelengths of each dye and after obtaining a standard calibration curve: 580 ± 20/625 ± 20 nm for FITC, 480 ± 15/530 ± 25 nm for TexasRed, and 675 ± 10/740 ± 40 nm for Alexa 680. The concentration–time curves of all dyes were fitted for each experiment separately with a monoexponential function. A retention ratio (RR) of the dye was calculated as follows: RR = final concentration at 30 minutes/initial concentration at 2 minutes.

For total intravascular blood volume (TBV) determination, the concentration of Albumin-Alexa 680 was determined at time = 2 minutes after bolus injection according to the following calculation: TBV (mL) = ([Albumin-Alexa syringe] × 0.1)/(Albumin-Alexa plasma).

Evans Blue Dye Technique. Evans blue is a fluorescent dye that readily binds to albumin once introduced intravascularly. The strong binding property of Evans blue dye (EBD) to serum albumin makes its escape from the vasculature to the tissue cells a well-established method for assessment of VBP.[23] A separate series of experiment (n = 12) was performed to determine albumin-bound EBD extravasation in the lung, heart, liver, and kidney in control, crystalloid-, and colloid-resuscitated groups. At the end of the experiment, 1 mL/kg BW EBD 4% (Fluka; Sigma Aldrich, Zwijndrecht, the Netherlands) was injected intravenously. Thirty minutes after injection, the inferior vena cava was incised for exsanguination and evacuation of the dye, and the animal's body was flushed thoroughly with 0.9% NaCl containing heparin (100 U/mL) via the femoral artery and jugular vein, until the fluid leaving was clear. At least 100 mL were required. Each harvested organ was cut in small pieces, rinsed, weighed, and placed in 1:1 weight (mg)/volume (µL) ratios of 0.9% NaCl. Samples were homogenized for 5 minutes using a handheld homogenizer (Polytron 1200 E; Kinematica, Luzern, Switzerland). Trichloroacetic acid 50% (Sigma Aldrich, Zwijndrecht, the Netherlands) was added in a 3:1 ratio (volume [µL]/weight [mg]). The trichloroacetic acid/homogenates were centrifuged at 10,000*g* for 20 minutes to remove precipitates and tissue debris, and the supernatants were added to a 96-well plate (30 µL per well, each plate supplemented with 90 µL of 95% ethanol and thoroughly mixed by pipetting) for fluorescence spectroscopy (620/680 nm).[24] EBD was extracted from the tissue, expressed as micrograms per gram of tissue, and determined against a calibration curve fitted with a 5-parameter logistic equation.

Intravital Fluorescence Microscopy. A direct method for the measurement of VBP is by intravital fluorescent microscopy based on the quantitative visualization of

large fluorescent tracers (>70 kDa) escaping from the microvasculature through the endothelial barrier into the interstitium.[25] After injection of this fluorescent dye, the time-dependent fluorescence intensity change in the vessel and in the surrounding tissue can be used to quantify VBP. In a second set of animals (n = 17), intravital fluorescence microscopy was used as described elsewhere[26] to measure extravasation of fluorescently labeled dextran (FITC-70 kDa dextran 10 mg/mL, 46,945; Sigma-Aldrich) as a model for macromolecular leakage and to determine extravascular accumulation. The setup of the experiment was exactly the same (NTHS, method of dye injection, muscle exposure) except that the handheld microscope was replaced by a fluorescence microscope. The microscopy setup consisted of a stereo fluorescence microscope (model M165 FC; Leica Microsystems, Wetzlar, Germany) equipped with a Peltier-cooled DFC420C color camera, a Planapo 1.0× objective lens, a 0.5× video objective (C-mount), 0.73× optical zoom, filter sets for bright field (420 nm cut on filter), fluorescence microscopy (excitation wavelength = 470 ± 20 nm, emission wavelength = 515 nm long pass), and a Leica EL6000 light source. The adjustable settings for fluorescence imaging were camera exposure time of 10 seconds, camera gain of 10, saturation of 1.0, gamma of 0.78, and light source setting of 5 (maximum). The camera was white balanced before every experimental session, and the hardware settings were kept constant throughout the entire experiment.

Before infusion of FITC-dextran, a bright field image was made of the region of interest, as well as a BL fluorescence image. After a 100-µL infusion over 1 minute, fluorescence images were acquired at 2, 5, 10, 15, 20, 25, and 30 minutes.

Images were analyzed in ImageJ software (National Institutes of Health, Bethesda, MD) for FITC fluorescence intensity as a measure of leakage and extravascular accumulation of dextran. Images were split into red-green-blue images, and the integrated density was calculated in the green channel. The fluorescence intensity was normalized to BL fluorescence and plotted as a fold increase for every postinfusion time point.

Tissue Edema. Edema formation may occur after accumulation of water as a result of vascular barrier compromise. At the end of the experiment, the heart, brain, kidney, lung, and liver were harvested to determine their water content using the wet/dry weighing technique (held at 100°C for 24 hours) and were calculated as follows: wet tissue weight/dry tissue weight ratio. This technique allows the measurement of water content in the organ.

Statistical Analysis

Values are expressed as mean ± SD when normally distributed (Kolmogorov–Smirnov test) or as median (interquartile range) otherwise. Repeated-measures 2-way analysis of variance (2 factors: time as a related within-animal factor and group as a between-animal factor) with post hoc Bonferroni correction test for multiple analysis was used to determine intergroup and/or intragroup differences of hemodynamic, microcirculation, biochemical data, glycocalyx degradation biomarkers, and intravital fluorescence microscopy. When significant interaction was observed between time and group, we reported simple main effects of group (type of fluid) compared to the control group at each timepoint and the simple main effect of time versus BL within the same group. Ordinary 1-way analysis of variance with Bonferroni correction was used for the analysis of TBV, tissue edema (organ by organ), urine output, and fluorescent tracer RRs. The decays in plasma concentration of fluorescent dyes at each timepoint were fitted with an exponential 1-phase decay using the least squares methods. Because of their non-Gaussian distribution, the analyses of power of exponential decay times fitting curves of each fluorescent dye and EBD concentrations within organs were performed using a Kruskal–Wallis test with a Dunn correction test. Statistical analysis was performed using GraphPad Prism version 7.0a for Mac (GraphPad Software, La Jolla, CA). The overall significance level for each hypothesis was .05. Adjusted *P* values were reported throughout the manuscript in post hoc tests.

Based on a previous study by Bansch et al,[27] we postulated that fluid resuscitation with crystalloids after hemorrhage will increase the plasma volume by approximately 25% to target an MAP of ≥80 mm Hg. Sample size was calculated by nQuery Advisor (Statistical Solutions Ltd, Boston, MA). A sample size of 6 in each group will have 80% power to detect a difference in means of −9.40 mL/kg (36.1 vs 45.5 mL/kg) assuming that the hemorrhagic shock group SD, σ1, is 2.700 and the balanced crystalloid group SD, σ2, is 6.200 (ratio of group 2 to group 1 SD is 2.296) using a 2-group Satterthwaite *t* test with a .050 two-sided significance level.

RESULTS

A total of 59 animals were included in this study: 30 rats for the predefined study, 17 rats for the second set of experiments, and 12 rats for the study with EBD. No animals died during the experiment. Hemodynamic parameters are presented in the Table. MAP and femoral artery blood flow significantly decreased during hemorrhagic shock. Shock-induced metabolic acidosis was associated with hyperlactatemia (>5 mmol·L^{-1}) compared to controls ($F_{[4,25]}$ = 11.52; P < .0001). The mean blood withdrawal was 5.7 ± 0.6 mL (17.1 ± 2 mL·kg^{-1} BW), corresponding to 27.5% ± 3.2% of total blood volume (BV) of the rats when calculated according to the following formula: BV (mL) = 0.06 × BW + 0.77.[28]

The total fluid resuscitation volumes were 63 mL (48–70 mL), 41.5 mL (36–45.2 mL), and 6.5 mL (5.7–12.2 mL) for the 0.9% NaCl, balanced crystalloid, and colloid groups, respectively ($F_{[2,16]}$ = 64.85; P < .0001). Fluid resuscitation induced a significant decrease in hemoglobin levels (Supplemental Digital Content 2, Table 1, http://links.lww.com/AA/C641). The associated urine output during the hour after fluid resuscitation was significantly higher in balanced crystalloid and 0.9% NaCl groups compared to controls, 0.067 mL·g^{-1}·hour^{-1} (0.056–0.094 mL·g^{-1}·hour^{-1}) (mean difference, −0.0587; 95% confidence interval [CI], −0.0986 to −0.0187; adjusted P = .0038) and 0.088 mL·g^{-1}·hour^{-1} (0.058–0.14 mL·g^{-1}·hour^{-1}) (mean difference, −0.0871; 95% CI, −0.1257 to −0.0484; adjusted P = .0001) vs 0.031 mL·g^{-1}·hour^{-1} (0.019–0.044 mL·g^{-1}·hour^{-1}), respectively (Supplemental Digital Content 3, Figure 2, http://links.lww.com/AA/C642). No urine was produced in the hemorrhagic shock group. The MAP was significantly lower in the fluid resuscitated groups compared to the control

Table. Hemodynamic Parameters and Lactate for Animals Resuscitated With Either Balanced Crystalloid, Balanced HES, or Normal Saline

	BL	T1	T2	T3
MAP (mm Hg)				
Control	91 ± 7	99 ± 7[a]	105 ± 6[a]	115 ± 6[a]
Hemorrhagic shock	97 ± 9	32 ± 2[a,b]	31 ± 2[a,b]	25 ± 4[a,b]
Balanced crystalloid	100 ± 8	32 ± 2[a,b]	85 ± 6[a,b]	81 ± 3[a,b]
Balanced HES	97 ± 8	33 ± 2[a,b]	101 ± 13	88 ± 11[a,b]
0.9% NaCl	90 ± 6	33 ± 2[a,b]	76 ± 4[a,b]	77 ± 7[a,b]
CVP (mm Hg)				
Control	5 ± 1	5 ± 1	5 ± 1	5 ± 1
Hemorrhagic shock	5 ± 1	5 ± 2	4 ± 2	5 ± 2
Balanced crystalloid	5 ± 1	5 ± 1	7 ± 1	7 ± 1
Balanced HES	6 ± 1	6 ± 1	8 ± 1*[a]	8 ± 1*[a]
0.9% NaCl	5 ± 2	6 ± 2	8 ± 2*[a]	8 ± 3*[a]
FABF (mL·minute^{-1})				
Control	2.4 ± 0.1	1.8 ± 0.1	2.3 ± 0.3	2.5 ± 0.2
Hemorrhagic shock	2.8 ± 0.3	1.6 ± 0.5[a]	1.2 ± 0.4[a,b]	1.1 ± 0.6[a,b]
Balanced crystalloid	2.3 ± 0.5	0.8 ± 0.4[a,b]	2.7 ± 0.7	3 ± 1.4
Balanced HES	2.5 ± 0.3	1.2 ± 0.8[a]	3 ± 0.6	3.7 ± 1
0.9% NaCl	2.2 ± 0.5	1.1 ± 0.4[a]	2.4 ± 0.7	2.3 ± 0.3
Lactate (mmol·L^{-1})				
Control	1.2 ± 0.1	1.7 ± 0.1	1.7 ± 0.2	1.7 ± 0.1
Hemorrhagic shock	1.2 ± 0.4	4.5 ± 1[a,b]	4.6 ± 1.3[a,b]	5.9 ± 1[a,b]
Balanced crystalloid	1.4 ± 0.3	5.1 ± 0.9[a,b]	3.6 ± 0.7[a,b]	2.2 ± 0.7
Balanced HES	1.4 ± 0.2	5.2 ± 1.2[a,b]	2.9 ± 0.8[a,b]	1.6 ± 0.5
0.9% NaCl	1.4 ± 0.4	5.7 ± 1.7[a,b]	3 ± 0.8[a,b]	1.3 ± 0.2

Differences between groups at the different time points were evaluated using the repeated-measures 2-way ANOVA with Bonferroni correction to adjust for multiple comparisons. Values are represented as means ± SD, n = 6 per group.

Abbreviations: ANOVA, analysis of variance; BL, baseline; CVP, central venous pressure; FABF, femoral artery blood flow; HES, hydroxyethyl starch; MAP, mean arterial pressure; NaCl, normal saline; SD, standard deviation.

[a]Adjusted $P < .05$ versus control group.

[b]$P < .05$ versus baseline value within the same group.

group at the end of the experiment. Strategies of fluid resuscitation with balanced crystalloid or colloid were both efficient in correcting pH and plasma lactate levels (Supplemental Digital Content 2, Table 1, http://links.lww.com/AA/C641) compared to normal saline.

Shedding Products of Glycocalyx Constituents

Glycocalyx shed products (hyaluronan, syndecan-1, and heparan) were all upregulated as a result of NTHS. Syndecan-1 levels (Figure 1A) were significantly increased in controls (mean difference, −788.7; 95% CI, −1456 to −121.1; adjusted $P = .015$), nonresuscitated hemorrhagic shock (mean difference, −1668; 95% CI, −2336 to −1001; adjusted $P < .0001$), balanced crystalloid (mean difference, −964.2; 95% CI, −1492 to −436.4; adjusted $P = .0001$), and HES (mean difference, −1030; 95% CI, −1594 to −465.8; adjusted $P = .0001$) groups at the end of the experiment (T3) compared to BL values. No changes in syndecan-1 were observed in the 0.9% NaCl group. Fluid resuscitation with balanced crystalloid (mean difference, 704; 95% CI, 163.8–1244; adjusted $P = .0067$), balanced HES (mean difference, 604.2; 95% CI, 49.43–1159; adjusted $P = .029$) solutions, or normal saline (mean difference, 1178; 95% CI, 623.7–1733; adjusted $P = .0001$) significantly reduced levels of syndecan-1 at the end of the experiment compared to the nonresuscitated hemorrhagic shock group. Hyaluronan levels (Figure 1B) were significantly higher at the end of the experiment in the nonresuscitated hemorrhage (mean difference, −923.1; 95% CI, −1216 to −630; adjusted $P = .0001$) and balanced crystalloid (mean difference, −1039; 95% CI, −1332 to −745.5; adjusted $P = .0001$) or HES (mean difference, −394.2; 95% CI, −670.1 to −118.3; adjusted $P = .0027$) groups compared to controls. The increase in glycocalyx shedding products was persistent after fluid resuscitation except for the hyaluronan component, which was decreased after balanced HES and normal saline administration. Heparan sulfate levels remained higher regardless of the resuscitation regimen or the absence of fluid resuscitation ($P < .001$) when compared to the controls (Figure 1C).

Microcirculatory Changes in Muscle

The microcirculatory parameters in the biceps femoris are represented in Figure 2. TVD, MFI, and PVD were not different after fluid resuscitation with either balanced crystalloid or colloid ($P > .05$). However, these same parameters were significantly altered in the normal saline (mean difference, 4.092; 95% CI, 0.6195–7.564; adjusted $P = .016$) and hemorrhagic shock (mean difference, 5.022; 95% CI, 1.55–8.495; adjusted $P = .0024$) groups when compared to the control group. The same parameters of these 2 latter groups were also significantly decreased compared to their BL values ($P < .05$).

Vascular Barrier Permeability

Fluorescent Tracer Decays and RRs. The decay times of fluorescent tracers are presented in Supplemental Digital Content 4, Figure 3, http://links.lww.com/AA/C643. The rate of disappearance can be given by the power of the exponential fit of the tracer curves provided for different groups. No significant alteration in this power was observed among the different groups. When considering the decrease

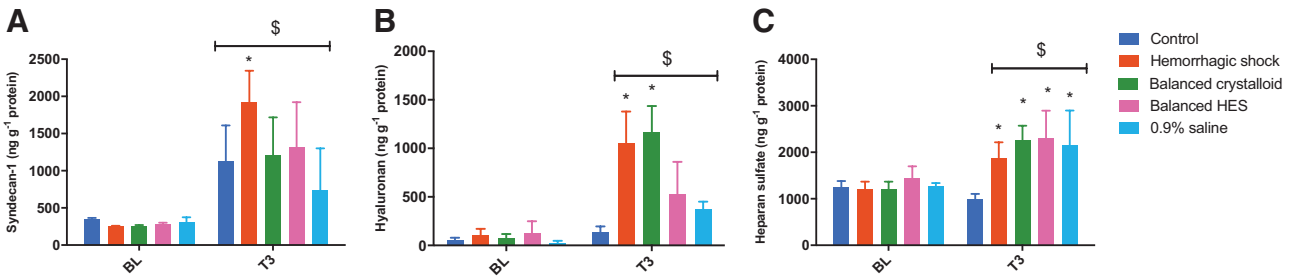

Figure 1. Plasma levels of syndecan-1 (A), hyaluronan (B), and heparan sulfate (C) during the experiment. Increased glycocalyx shedding persists after fluid resuscitation except for the hyaluronan component, which is decreased with balanced hydroxyethyl starch (HES) resuscitation. Repeated-measures 2-way analysis of variance test used with Bonferroni correction to adjust for multiple comparisons. *Adjusted $P < .01$ versus control group at the same time point, $\$P < .05$ versus baseline (BL) value within the same group (n = 6–8/group).

in normalized concentrations at each time point per group of fluid resuscitation (Supplemental Digital Content 5, Figure 4, http://links.lww.com/AA/C644), a significant difference was present between FITC 500-kDa and Texas Red-40 kDa dextrans ($P < .05$), suggesting a different escape rate from the vascular system according to molecular size. Albumin-Alexa 680 and FITC 500 kDa showed similar decays regardless of the group, proving that these dyes did not cross the vascular barrier.

The RR of different dyes bound to different molecular sizes is presented in Figure 3. No significant differences were noted.

EBD Technique. The EBD extraction from tissues is presented in Supplemental Digital Content 6, Figure 5, http://links.lww.com/AA/C645 (n = 4 per group, excluding nonresuscitated NTHS and normal saline groups). A broad variability in the pulmonary EBD concentration was observed. No differences were noted in the other organs between control and resuscitated animals regardless of the fluid chosen.

Fluorescence Intravital Microscopy. Figure 4A is an example of the time course of fluorescence escaping through the microvasculature obtained with intravital fluorescence microscopy in animals undergoing NTHS resuscitation with different fluids or the control. The fluorescence levels did not significantly differ from the control group. As a damage positive control for vascular barrier disruption, hyperthermia (temperature >42°C) was induced in a rat. The time course of the relative increase in fluorescence is displayed in Figure 4B. We did not include a nonresuscitated hemorrhagic shock group in this setting because we did not see any significant leakage after fluid resuscitation of hemorrhagic shock in the other groups. Leakage was unlikely to happen, and the experiment was considered futile and not in accordance with the local animal ethic committee.

Tissue Edema. The quantification of tissue edema in different organs (lung, brain, liver, kidney, and heart) is presented in Supplemental Digital Content 7, Figure 6, http://links.lww.com/AA/C646. Although the wet/dry ratio may be different among organs, no significant tissue edema was present after fluid resuscitation compared to the control group. Nonresuscitated hemorrhagic shock animals exhibited a significantly smaller wet-to-dry weight ratio in the liver compared to control (mean difference, 0.373; 95% CI, 0.03158–0.7151; adjusted $P = .029$). In addition, no difference was noted between balanced crystalloid and colloid fluid resuscitation with regard to tissue edema.

Total Intravascular BV

The TBV was reduced in the nonresuscitated hemorrhagic shock group (15.2 ± 1.3 mL) compared to the control group (17.5 ± 1.3 mL) (mean difference, 2.3; 95% CI, 0.20–4.5; $P = .027$; Figure 5). Fluid resuscitation increased TBV significantly in the balanced crystalloid group (21.1 ± 1.1 mL) compared to the control and hemorrhagic shock groups (mean difference, –3.6; 95% CI, –5.7 to –1.5; adjusted $P < .0001$, and –5.9; 95% CI, –8.07 to –3.9; adjusted $P < .0001$, respectively).

DISCUSSION

The main result of our study has been the demonstration that in NTHS, glycocalyx degradation occurs but is not associated with an increased VBP. Furthermore, our results show that glycocalyx degradation and microcirculatory alterations persist after fluid resuscitation independent of its composition. However, fluid resuscitation alone does not result in a change in VBP and in its extension tissue edema. These results on changes in VBP were demonstrated using 4 independent techniques. However, some differences remain regarding the nature of glycocalyx shedding products, as indicated by the biomarkers profile differing between resuscitation fluids. Normal saline was found to be the less-suitable fluid because it restored neither the microcirculatory alterations nor the acid-base balance. These results stress the complexity of VBP regulation in the context of hemorrhagic shock and identify a gradation of vascular injury. A partial shedding of the glycocalyx either NTHS induced or following fluid resuscitation did not impair vascular barrier competence. This result challenges the role of the glycocalyx as a major contributor of the VBP.

It is assumed that the glycocalyx shedding is a direct cause of an increase in VBP. Glycocalyx-shedding products are often considered as surrogate markers of vascular permeability. Most of the data regarding the relationship between glycocalyx shedding and increased VBP come from ex vivo isolated organ experiments or in vivo enzymatic degradation treatments. However, these models have serious shortcomings and ignore a large part of the pathophysiological pathways occurring in response to shock.[19,29] Thus,

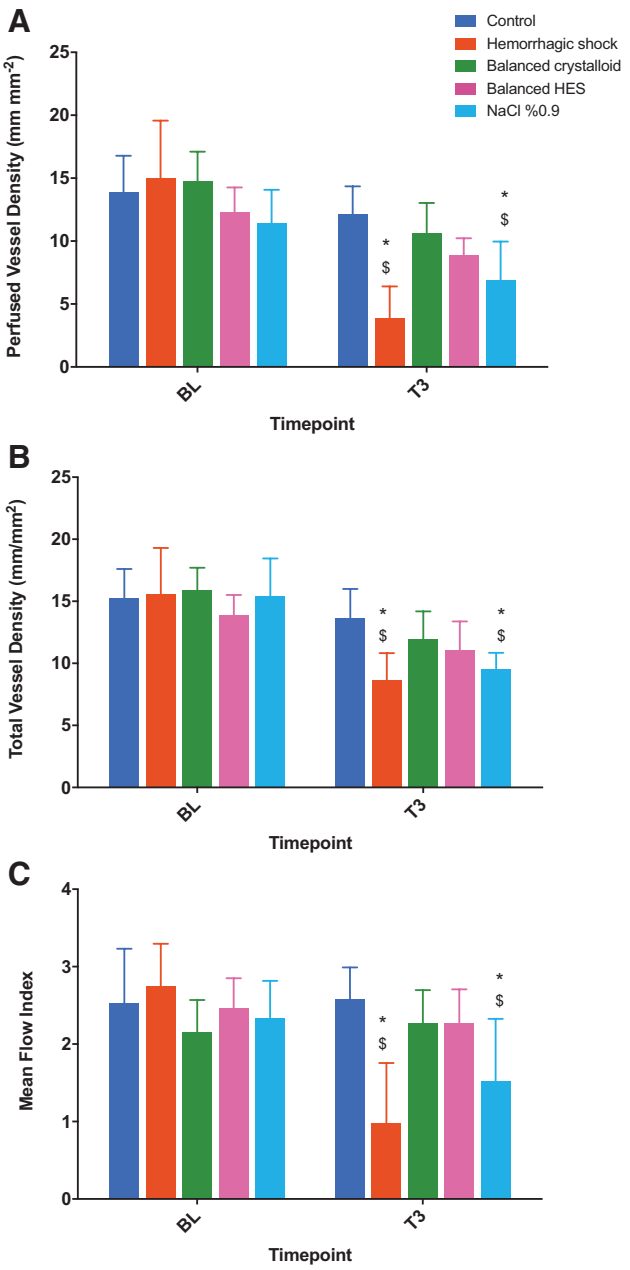

Figure 2. Microcirculatory parameters assessed at a single spot of the biceps femoris with handheld intravital microscopy. Despite normal mean arterial pressure, the microcirculation is not fully restored after fluid resuscitation when considering the total vessel density. Repeated-measures 2-way analysis of variance test used with Bonferroni correction to adjust for multiple comparisons. *Adjusted $P < .05$ versus control group at the same time point, $\$P < .05$ versus Baseline (BL) value within the same group (n = 8/group). HES indicates hydroxyethyl starch; NaCl, normal saline.

the results of these experiments may not be relevant to physiological situations. Rehm et al,[19] in an isolated heart model, first introduced the concept of a "double barrier" where the glycocalyx can be enzymatically erased while the endothelial cells remain untouched, without causing significant effects on coronary permeability. Our results support these findings, although we observed microcirculatory alterations related to hemorrhagic shock. These microcirculatory disturbances are usually a marker of endothelial cell dysfunction. In an hamster window chamber model, Landsverk et al[30] observed a significant decrease in functional capillary density after hyaluronidase injection without associated vascular leakage. The authors reported a 50- to 100-fold increase in plasma levels of hyaluronan, suggesting an efficient glycocalyx degradation. In another study, Bansch et al[27] did not observe any leak of radiolabeled albumin in an acute model of hemorrhage 4 hours after resuscitation with either Ringer's acetate or 5% albumin, suggesting an intact microvascular barrier, bearing out our results.

Similarly to other authors, we demonstrated that NTHS did injure the different endothelial glycocalyx components, and fluid resuscitation after hemorrhage may alter glycocalyx components in different ways.[6,13,14,31] However, the level of injury may vary according to the model used, the duration of shock, or the vascular bed under observation. In a rodent model of hemorrhagic shock, Kozar et al[13] showed that lung injury was markedly increased with decreased cell surface syndecan-1 expression in pulmonary alveolar cells after lactated Ringer's resuscitation. On the contrary, fresh frozen plasma (FFP) restored in part the shed glycocalyx. Direct assessment of VBP was, however, not performed in this experiment, nor were tissue edema measurements (wet/dry ratio). Torres Filho et al[6,14,15] published several experimental studies of NTHS in rats, where microvascular permeability in the cremaster muscle was increased in association with glycocalyx degradation after fluid resuscitation with crystalloids compared to FFP or whole blood. In these studies, VBP was assessed in 1 vascular bed (cremaster), which had been surgically prepared and may have induced local inflammation. Other than this difference, animals were subjected to a fixed relative volume hemorrhage (40% of total BV) and were fluid resuscitated with empirical amounts not matching clinical practice, which usually targets a macrocirculatory end point. These authors showed a positive correlation between changes in microvascular permeability and in glycocalyx-shedding products (plasma syndecan-1 and heparan sulfate).[15] The discrepancies with other studies may lie in the fact that we undertook a multifaceted approach of the VBP. We did not focus on a specific vascular bed that might be more sensitive to hyperpermeability but rather took into consideration the whole cardiovascular system and different organs. Moreover, the glycocalyx has a remarkable heterogeneous distribution within organs. Finally, compared to other authors, the duration of our hemorrhagic shock and fluid resuscitation observation time periods were shorter, 60 vs 90 minutes and 1 vs 3 hours, respectively.[13,32]

An intact glycocalyx is a prerequisite for normal vascular physiology, and each component exhibits a unique function. Many of its components are essential for homeostasis,[33,34] mechanosensors for flow-mediated shear stress and autoregulation,[1,33] and leukocyte–endothelial cell interactions.[35] Glycocalyx shedding could be an essential and normal response to injury and could be appropriate or even beneficial. Could preventing glycocalyx shedding even be harmful?[36] Its degradation occurs in a wide range of conditions, such as diabetes/hyperglycemia,[9] atherosclerosis and hypertension,[4] sepsis,[8,37] reperfusion injury,[38] or smoking.[39] Whether glycocalyx shedding alone causes tissue edema or capillary leakage

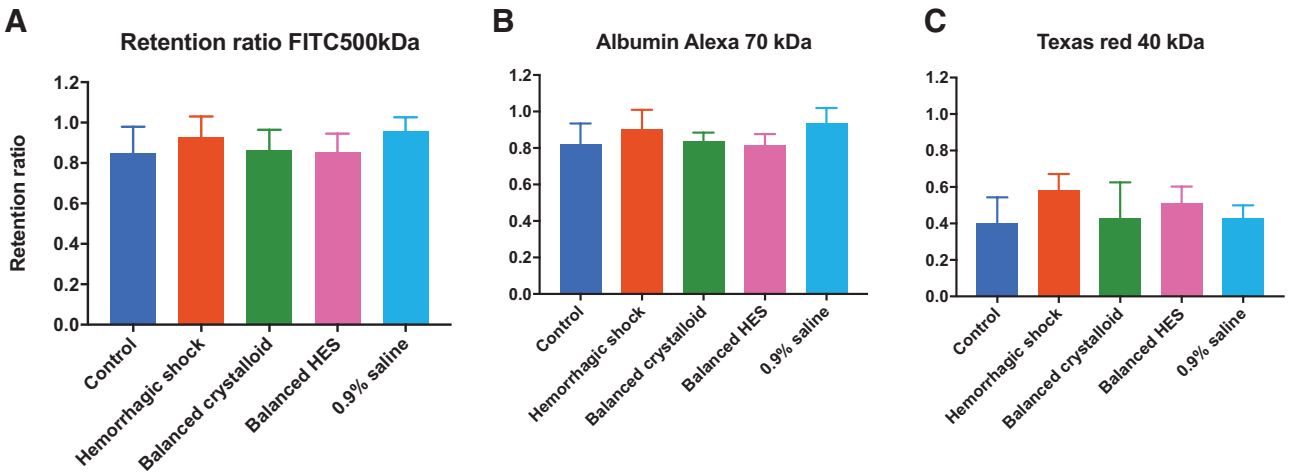

Figure 3. Retention ratio of the different tracers expressed as the ratio between the final (at 30 min) and initial concentrations (at 2 min) of the dye. One-way analysis of variance test used for each fluorescent dye with Bonferroni correction to adjust for multiple comparisons (n = 6/group). FITC indicates fluorescein isothiocyanate; HES, hydroxyethyl starch.

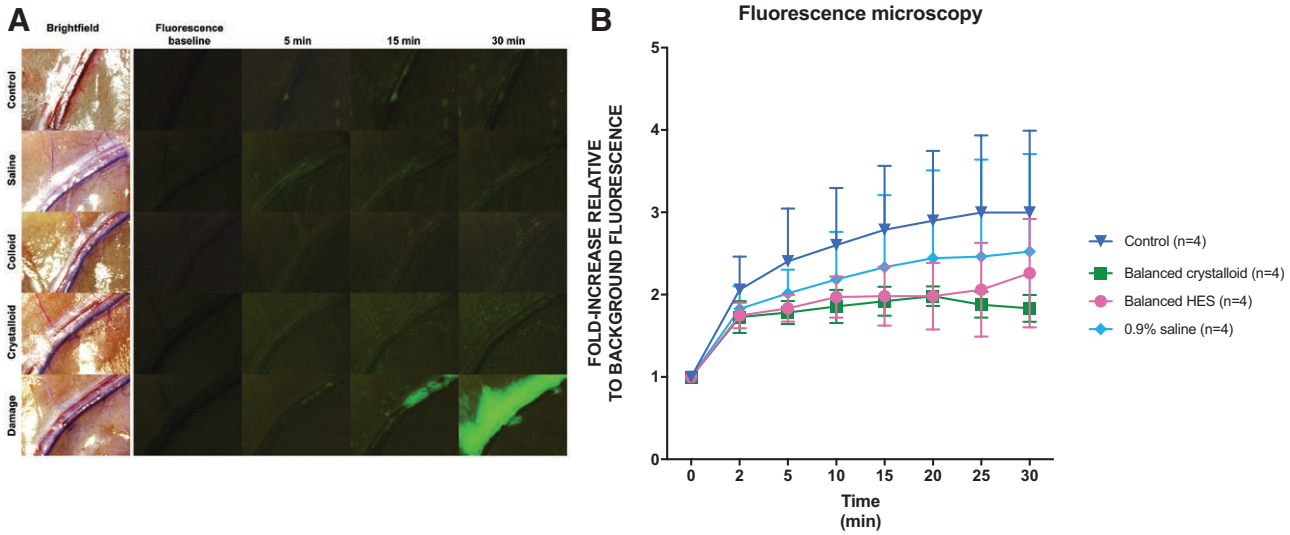

Figure 4. Fluorescence microscopy of the microcirculation of the right biceps femoris. A, Time course of fluorescence imaging at different time points after dye infusion. B, Increase in fluorescence relative to background during the 30 min after injection. Infusion of 100 µL fluorescein isothiocyanate-70 kDa dextran (10 mg/mL) and subsequent fluorescence images at 2, 5, 10, 15, 20, 25, and 30 min. For the sake of clarity, only baseline, 5-, 15-, and 30-min time points are shown. The hemorrhagic shock group was not determined. Repeated-measures 2-way analysis of variance test used with Bonferroni correction to adjust for multiple comparisons. HES indicates hydroxyethyl starch.

remains controversial. We suggest that, although the glycocalyx is essential from a functional point of view, it is not a key component of the permeability of the vascular barrier. The traditional Starling's law has been revised several times, taking into account not only the glycocalyx but also the most significant components, such as the endothelial cell junctions, the basement membrane, and pericytes.[3,40,41]

In light of the literature and our data, a hierarchy of vascular injury can be proposed, initiated by glycocalyx shedding followed by microcirculatory alterations and, ultimately if injury persists or induces major inflammation, by a loss of VPB and tissue edema. This concept of graded injury, although intuitive, would need further investigation in different models and vascular beds. Only the most severe models, using degradative enzymes or sustained sepsis, such as cecal ligation and puncture, where other components of the vascular barrier (eg, adherens junctions/cadherins) become compromised, have shown vascular leakage and tissue edema.[16,17,41,42] In the present model, this level of vascular injury was not achieved.

Due to the large amount of crystalloids used for fluid resuscitation, one was expecting to observe fluid accumulation within various organs. Although crystalloids inevitably accumulate in tissues when given in large amounts, such findings do not necessarily imply VBP alterations.[43] In our experiment, balanced crystalloid or normal saline markedly increased urine output. Between a third and a half of the resuscitation volume administered was promptly excreted (<1 hour). Few experimental studies have focused on urine output during fluid resuscitation in hemorrhagic shock, and the results were consistent with ours.[44] While we did not observe an overall increase in VBP or tissue edema in the lung, brain, liver, kidney, or heart, it might be possible that

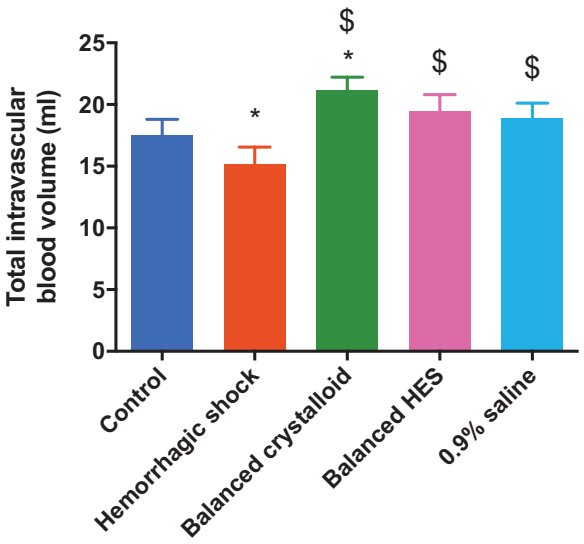

Figure 5. Total intravascular blood volume at the end of the experiment as determined by Albumin-Alexa 680 fluorimetry. *Adjusted $P <$ .05 versus control, $adjusted $P <$ .001 versus hemorrhagic shock. One-way analysis of variance test used with Bonferroni correction to adjust for multiple comparisons (n = 6/group). HES indicates hydroxyethyl starch.

fluid in excess tends to accumulate in the intestinal mucosae and mesentery, muscles, or skin.

In our study, balanced HES solution administered after NTHS markedly decreased the level of hyaluronan compared to balanced crystalloid. However, Nelson et al[31] noted that a decrease in glycocalyx-shedding biomarkers may be related to a dilutional effect induced by the volume expander effect of colloids or FFP. Torres et al[15,45] did not notice any beneficial effect of high molecular weight starch on plasma syndecan-1 levels or in vivo glycocalyx thickness after fluid resuscitated hemorrhagic shock. To date, there is no evidence that restoring the glycocalyx in the context of jeopardized VBP would be beneficial or would help reduce capillary leakage when already present.

Limitations of the Study

Due to a limited number of animals per group, the reproducibility of certain techniques may be questioned; however, the results were consistent in each group among different techniques that analyzed the VBP. In such a heavily instrumented model, it is difficult to control all of the factors that may induce glycocalyx shedding. Surgery and fluid maintenance, similar in all groups, may have induced some glycocalyx degradation, as indeed observed in the control group. NTHS could have been prolonged for several hours, but would have been at variance with clinical practice in operating or emergency rooms. We did not investigate the mechanisms behind glycocalyx shedding, such as oxidative stress and inflammation. Our technique of microcirculation measurements did not allow leukocyte–endothelium interaction analyses because of the high velocity of these cells due to hemodilution.

CONCLUSIONS

This study is the first to provide an integrative assessment of the VBP, including macro and microhemodynamic monitoring, glycocalyx shedding, and vascular leakage, in a clinically relevant model of NTHS. NTHS induced glycocalyx shedding and microcirculatory modifications, but these were not associated with increased VBP after fluid resuscitation. These results challenge the concept of glycocalyx as a key determinant of vascular permeability. The endothelial cell junctions may be a more important contributor to the VBP.[41]

DISCLOSURES

Name: Philippe Guerci, MD.
Contribution: This author helped design the study, carry out the experiments, analyze the data, write the first draft and final version, and review the manuscript.
Conflicts of Interest: None.
Name: Bulent Ergin, PhD.
Contribution: This author helped design the study, carry out the experiments, analyze the data, write the first draft and final version, and review the manuscript.
Conflicts of Interest: None.
Name: Zuhre Uz, MD.
Contribution: This author helped analyze the data (microcirculation clips) and review the manuscript.
Conflicts of Interest: None.
Name: Yasin Ince, MSc.
Contribution: This author helped analyze the data (microcirculation clips) and review the manuscript.
Conflicts of Interest: None.
Name: Martin Westphal, MD, PhD.
Contribution: This author helped analyze the data (microcirculation clips) and review the manuscript.
Conflicts of Interest: M. Westphal is the Chief Medical Officer of Fresenius Kabi AG.
Name: Michal Heger, PhD.
Contribution: This author helped carry out experiments, analyze the data, write the first draft, and review the manuscript.
Conflicts of Interest: None.
Name: Can Ince, PhD.
Contribution: This author helped design the study, analyze the data, write the final version, and review the manuscript.
Conflicts of Interest: C. Ince runs an Internet site (microcirculationacademy.org) which offers services (eg, training, courses, and analysis) related to clinical microcirculation and has received honoraria and independent research grants from Fresenius Kabi, Baxter Health Care, and AM-Pharma; has developed sidestream dark field imaging; is listed as an inventor on related patents commercialized by MicroVision Medical under a license from the Academic Medical Center; and has been a consultant for MicroVision Medical in the past but has not been involved with this company for more than 5 years. The company that developed the CytoCam-incident dark field imaging system, Braedius Medical, is owned by a relative of C. Ince. C. Ince has no financial relationship with Braedius Medical (ie, never owned shares or received consultancy or speaker fees).
This manuscript was handled by: Alexander Zarbock, MD.

REFERENCES

1. Weinbaum S, Tarbell JM, Damiano ER. The structure and function of the endothelial glycocalyx layer. *Annu Rev Biomed Eng*. 2007;9:121–167.
2. Curry FE, Adamson RH. Endothelial glycocalyx: permeability barrier and mechanosensor. *Ann Biomed Eng*. 2012;40:828–839.
3. Woodcock TE, Woodcock TM. Revised starling equation and the glycocalyx model of transvascular fluid exchange: an improved paradigm for prescribing intravenous fluid therapy. *Br J Anaesth*. 2012;108:384–394.
4. Tarbell JM, Cancel LM. The glycocalyx and its significance in human medicine. *J Intern Med*. 2016;280:97–113.
5. Chignalia AZ, Yetimakman F, Christiaans SC, et al. The glycocalyx and trauma: a review. *Shock*. 2016;45:338–348.
6. Torres Filho I, Torres LN, Sondeen JL, Polykratis IA, Dubick MA. In vivo evaluation of venular glycocalyx during hemorrhagic shock in rats using intravital microscopy. *Microvasc Res*. 2013;85:128–133.

7. Ince C, Mayeux PR, Nguyen T, et al; ADQI XIV Workgroup. The endothelium in sepsis. *Shock*. 2016;45:259–270.
8. Chelazzi C, Villa G, Mancinelli P, De Gaudio AR, Adembri C. Glycocalyx and sepsis-induced alterations in vascular permeability. *Crit Care*. 2015;19:26.
9. Zuurbier CJ, Demirci C, Koeman A, Vink H, Ince C. Short-term hyperglycemia increases endothelial glycocalyx permeability and acutely decreases lineal density of capillaries with flowing red blood cells. *J Appl Physiol (1985)*. 2005;99:1471–1476.
10. Miranda CH, de Carvalho Borges M, Schmidt A, Marin-Neto JA, Pazin-Filho A. Evaluation of the endothelial glycocalyx damage in patients with acute coronary syndrome. *Atherosclerosis*. 2016;247:184–188.
11. Chappell D, Bruegger D, Potzel J, et al. Hypervolemia increases release of atrial natriuretic peptide and shedding of the endothelial glycocalyx. *Crit Care*. 2014;18:538.
12. Kataoka H, Ushiyama A, Akimoto Y, Matsubara S, Kawakami H, Iijima T. Structural behavior of the endothelial glycocalyx is associated with pathophysiologic status in septic mice: an integrated approach to analyzing the behavior and function of the glycocalyx using both electron and fluorescence intravital microscopy. *Anesth Analg*. 2017;125:874–883.
13. Kozar RA, Peng Z, Zhang R, et al. Plasma restoration of endothelial glycocalyx in a rodent model of hemorrhagic shock. *Anesth Analg*. 2011;112:1289–1295.
14. Torres LN, Chung KK, Salgado CL, Dubick MA, Torres Filho IP. Low-volume resuscitation with normal saline is associated with microvascular endothelial dysfunction after hemorrhage in rats, compared to colloids and balanced crystalloids. *Crit Care*. 2017;21:160.
15. Torres Filho IP, Torres LN, Salgado C, Dubick MA. Plasma syndecan-1 and heparan sulfate correlate with microvascular glycocalyx degradation in hemorrhaged rats after different resuscitation fluids. *Am J Physiol Heart Circ Physiol*. 2016;310:H1468–H1478.
16. VanTeeffelen JW, Brands J, Janssen BJ, Vink H. Effect of acute hyaluronidase treatment of the glycocalyx on tracer-based whole body vascular volume estimates in mice. *J Appl Physiol (1985)*. 2013;114:1132–1140.
17. Gao L, Lipowsky HH. Composition of the endothelial glycocalyx and its relation to its thickness and diffusion of small solutes. *Microvasc Res*. 2010;80:394–401.
18. Cabrales P, Vázquez BY, Tsai AG, Intaglietta M. Microvascular and capillary perfusion following glycocalyx degradation. *J Appl Physiol (1985)*. 2007;102:2251–2259.
19. Rehm M, Zahler S, Lötsch M, et al. Endothelial glycocalyx as an additional barrier determining extravasation of 6% hydroxyethyl starch or 5% albumin solutions in the coronary vascular bed. *Anesthesiology*. 2004;100:1211–1223.
20. Donati A, Damiani E, Domizi R, et al. Alteration of the sublingual microvascular glycocalyx in critically ill patients. *Microvasc Res*. 2013;90:86–89.
21. Aykut G, Veenstra G, Scorcella C, Ince C, Boerma C. Cytocam-IDF (incident dark field illumination) imaging for bedside monitoring of the microcirculation. *Intensive Care Med Exp*. 2015;3:40.
22. Massey MJ, Shapiro NI. A guide to human in vivo microcirculatory flow image analysis. *Crit Care*. 2016;20:35.
23. Cooksey CJ. Quirks of dye nomenclature: 1–Evans blue. *Biotech Histochem*. 2014;89:111–113.
24. Wang HL, Lai TW. Optimization of Evans blue quantitation in limited rat tissue samples. *Sci Rep*. 2014;4:6588.
25. Kenne E, Lindbom L. Imaging inflammatory plasma leakage in vivo. *Thromb Haemost*. 2011;105:783–789.
26. Olthof PB, van Golen RF, Meijer B, et al. Warm ischemia time-dependent variation in liver damage, inflammation, and function in hepatic ischemia/reperfusion injury. *Biochim Biophys Acta Mol Basis Dis*. 2017;1863:375–385.
27. Bansch P, Statkevicius S, Bentzer P. Plasma volume expansion with 5% albumin compared to Ringer's acetate during normal and increased microvascular permeability in the rat. *Anesthesiology*. 2014;121:817–824.
28. Lee HB, Blaufox MD. Blood volume in the rat. *J Nucl Med*. 1985;26:72–76.
29. Bruegger D, Rehm M, Jacob M, et al. Exogenous nitric oxide requires an endothelial glycocalyx to prevent postischemic coronary vascular leak in guinea pig hearts. *Crit Care*. 2008;12:R73.
30. Landsverk SA, Tsai AG, Cabrales P, Intaglietta M. Impact of enzymatic degradation of the endothelial glycocalyx on vascular permeability in an awake hamster model. *Crit Care Res Pract*. 2012;2012:842545.
31. Nelson A, Statkevicius S, Schött U, Johansson PI, Bentzer P. Effects of fresh frozen plasma, Ringer's acetate and albumin on plasma volume and on circulating glycocalyx components following haemorrhagic shock in rats. *Intensive Care Med Exp*. 2016;4:6.
32. Pati S, Peng Z, Wataha K, Miyazawa B, Potter DR, Kozar RA. Lyophilized plasma attenuates vascular permeability, inflammation and lung injury in hemorrhagic shock. *PLoS One*. 2018;13:e0192363.
33. Reitsma S, Slaaf DW, Vink H, van Zandvoort MA, oude Egbrink MG. The endothelial glycocalyx: composition, functions, and visualization. *Pflugers Arch*. 2007;454:345–359.
34. Chappell D, Brettner F, Doerfler N, et al. Protection of glycocalyx decreases platelet adhesion after ischaemia/reperfusion: an animal study. *Eur J Anaesthesiol*. 2014;31:474–481.
35. Constantinescu AA, Vink H, Spaan JA. Endothelial cell glycocalyx modulates immobilization of leukocytes at the endothelial surface. *Arterioscler Thromb Vasc Biol*. 2003;23:1541–1547.
36. Hayashida K, Parks WC, Park PW. Syndecan-1 shedding facilitates the resolution of neutrophilic inflammation by removing sequestered CXC chemokines. *Blood*. 2009;114:3033–3043.
37. Schmidt EP, Yang Y, Janssen WJ, et al. The pulmonary endothelial glycocalyx regulates neutrophil adhesion and lung injury during experimental sepsis. *Nat Med*. 2012;18:1217–1223.
38. van Golen RF, Reiniers MJ, Vrisekoop N, et al. The mechanisms and physiological relevance of glycocalyx degradation in hepatic ischemia/reperfusion injury. *Antioxid Redox Signal*. 2014;21:1098–1118.
39. Ikonomidis I, Marinou M, Vlastos D, et al. Effects of varenicline and nicotine replacement therapy on arterial elasticity, endothelial glycocalyx and oxidative stress during a 3-month smoking cessation program. *Atherosclerosis*. 2017;262:123–130.
40. Kottke MA, Walters TJ. Where's the leak in vascular barriers? A review. *Shock*. 2016;46:20–36.
41. Goldenberg NM, Steinberg BE, Slutsky AS, Lee WL. Broken barriers: a new take on sepsis pathogenesis. *Sci Transl Med*. 2011;3:88ps25.
42. Chappell D, Jacob M. Role of the glycocalyx in fluid management: small things matter. *Best Pract Res Clin Anaesthesiol*. 2014;28:227–234.
43. Chawla LS, Ince C, Chappell D, et al; ADQI XII Fluids Workgroup. Vascular content, tone, integrity, and haemodynamics for guiding fluid therapy: a conceptual approach. *Br J Anaesth*. 2014;113:748–755.
44. Todd SR, Malinoski D, Muller PJ, Schreiber MA. Lactated Ringer's is superior to normal saline in the resuscitation of uncontrolled hemorrhagic shock. *J Trauma*. 2007;62:636–639.
45. Torres LN, Sondeen JL, Ji L, Dubick MA, Torres Filho I. Evaluation of resuscitation fluids on endothelial glycocalyx, venular blood flow, and coagulation function after hemorrhagic shock in rats. *J Trauma Acute Care Surg*. 2013;75:759–766.